Physical properties of individual anatase TiO_2 nanowires investigated by field emission in a transmission electron microscope

Jun Shen,[a] Pascal Vincent,[b] Nicholas P. Blanchard, Jimmy Nicolle, May Choueib, Stephen T. Purcell, and Philippe Poncharal
Université Claude Bernard, Lyon1, LPMCN, CNRS, UMR 5586, Université Lyon 1, Villeurbanne 69622, France

Vincent Salles and Arnaud Brioude
Université Claude Bernard, Lyon1, Laboratoire des Multimatériaux et Interfaces, UMR CNRS 5615, Villeurbanne 69622, France

(Received 8 June 2011; accepted 20 November 2011; published 13 December 2011)

The authors present studies on the field emission (FE) mechanism and the FE-induced transformation of individual anatase TiO_2 nanowires (NWs). The NWs were synthesized by electrospinning followed by calcination at 500 °C which produces polycrystalline anatase nanofibers as determined by Raman spectroscopy and transmission electron microscopy (TEM) characterization. Nanowires of ~100 nm in diameter were individually mounted at the apexes of tungsten tips for further physical characterization. The FE experiments were carried out in a TEM which allows the measurement of the FE current while simultaneously observing structural modifications leading to the NW's destruction. For low currents (below 100 nA), we observe reproducible FE Fowler-Nordheim I/V characteristics. Higher currents (up to 1 μA) can be obtained but sudden destruction of the NW may take place. Our observations show that a thermally-activated transition occurs and leads to rapid re-crystallization phenomena and a variation of the FE characteristics. If not controlled, this transition leads to thermal runaway and sample destruction. The understanding of the destruction phenomena is a key parameter to further improve the FE performance of such nanowire cathodes.
 [DOI: 10.1116/1.3668121]

I. INTRODUCTION

TiO_2 nanostructures are now attracting a lot of interest due to the combination of their large surface area and their potential applications in photocatalysis, self-cleaning coatings, sensors, smart surface coatings or solar cells. At the same time, many synthesis techniques have been developed to produce such TiO_2 nanostructures (0D and 1D), such as hydrothermal or solvothermal synthesis,[1] sol-gel template method,[2] or electrospinning.[3] More recently, the application of TiO_2 nanowires (NWs) as field emission (FE) sources has been explored due to their high aspect ratio and good FE properties. Experiments have been conducted on anatase[4] and rutile[5,6] nanowires produced by several techniques. These studies have been realized on macroscopic surfaces covered by NWs and current densities of up 1 mA/cm^2 have been reported.

However, there are still many open questions to reach the ultimate performance of these cathodes or to give insights to improve existing cathodes: what is the exact FE mechanism for these supposedly insulating nanowires (is it governed by surface leakages or bulk properties, e.g.), is there an ideal structure for FE (anatase or rutile, monocrystalline or polycrystalline, etc.), what is the maximum current that a NW can sustain before destruction and what is the destruction mechanism, etc.?

As an example, recent work on the FE of SiC semiconducting NWs has shown the importance of surface leakage currents (through contamination or overlayers, surface states, etc.) on the FE performance of an emitter.[7,8] For a given individual nanowire it has been shown that the presence of surface leakage currents leads to rather high FE currents and quasi-linear fowler-nordheim (FN) curves, while after cleaning the surface much lower currents were observed for the same voltages and the FN curves saturated for certain voltage ranges in accordance with theoretical models. To give insights into these questions, fundamental studies have to be conducted on individual nanowires.

In this paper, we present fundamental FE studies of individual anatase nanowires attached to the ends of etched tungsten tips. The FE experiments were carried out in a transmission electron microscope (TEM) to characterize the emission process, measure the maximum current of our sample and explore the destruction process of these nanowires.

II. TiO_2 NANOWIRE SYNTHESIS AND CHARACTERIZATION

In a typical synthesis procedure of TiO_2 nanowires, the polymeric solution was prepared using titanium isopropoxide ($Ti(OiPr)_4$, $C_{12}H_{28}O_4Ti$, 97% in purity, Aldrich) as the titanium precursor and polyvinylpyrrolidone (PVP, Aldrich, Mw _ 1 300 000) as an organic polymer to increase the spinnability of the starting solution. This solution containing 0.03 and 0.11 g/mL of PVP and $Ti(OiPr)_4$, respectively was then loaded into a plastic syringe equipped with a 21 gauge stainless steel needle. The high voltage (HV supply from Iseg Co., T1CP 300 304 p) was applied between this spinneret and a static metallic target (ground) placed 10 cm from

[a]Present address: Department of Electrical and Computer Engineering, University of British Columbia, Vancouver, BC, Canada V6Z 1T4.
[b]Author to whom correspondence should be addressed; electronic mail: pascal.vincent@univ-lyon1.fr

the needle tip. A continuous feeding rate of $0.8\,mL{\cdot}h^{-1}$ was controlled with a syringe pump (KDS-100, Bioseb Co.). Under these working conditions, an electric field of 1 kV/cm led to a stable jet. The electrospinning step was conducted in air in order to favor the hydrolysis of the Ti precursor into $Ti(OH)_4$ before a thermal treatment carried out at 500 °C for 4 h in air to convert the Ti hydroxide into TiO_2 and to remove the organic part from the wires.

Nanowires having diameters of ~100 nm, produced using the above method, were chosen for the FE studies. This diameter provides a good compromise between ease of handling of the nanowires, transparence to electrons for microstructure observations by TEM and reasonable macroscopic applied voltages for inducing FE at the nanowires' apex. Sample structure was characterized by SEM, TEM and Raman spectroscopy. Figure 1(a) shows an SEM image of as-spun $Ti(OiPr)_4$/PVP composite nanowires. Each single composite nanowire has a regular cylindrical shape, a smooth surface and an average diameter of about 200 ~ 300 nm. As the PVP was selectively removed by annealing the sample, the nanowires remained as continuous structures [Fig. 1(b)], with a reduced average diameter of 100–150 nm. This shrinkage is mainly due to loss of PVP and the organic part of the Ti-containing precursor.

Figure 1(c) shows the Raman spectra of the untreated and annealed bulk samples. While the untreated sample presents the spectrum of a noncrystalline material, the spectrum of the sample after annealing shows the typical Raman shifts analogous to those of pure crystalline anatase. The three bands at 634 (ν_1), 197 (ν_5), and 145 cm^{-1}(ν_6) are assigned to the Eg modes and the band at 394 cm^{-1} (ν_4) to the B_{1g} mode of the TiO_2 anatase phase. The band at 516 cm^{-1} is a doublet of the A_{1g} and B_{1g} modes of anatase TiO_2.[9,10]

Another way to characterize the nanofibers' structure is to determine the full width at half maximum (FWHM) of the anatase 144 cm^{-1} line. We have measured it to be ~15.4 cm^{-1}, clearly greater than the monocrystalline value of 7 cm^{-1}. Based on previous studies,[11] this value corresponds to a TiO_2 nanoparticle with a mean size of around 6 nm.

Figure 2(a) shows a TEM image of the samples after they had been calcined in air at 500 °C. This image indicates clearly that the wirelike morphology of the samples is retained after calcination but voids between adjacent nanoparticles appear due to the sintering of TiO_2 nanoparticles and the removal of the polymer. Figure 2(b) shows the high-resolution TEM (HRTEM) image of a nanowire after calcination which indicates that the TiO_2 nanowires have a polycrystalline structure throughout their length with TiO_2 nanoparticles stacking around and on top of each other, which is further corroborated by the selected area electron diffraction (SAED) pattern in Fig. 2(c). The size of these nanoparticles is close to that estimated by Raman spectroscopy.

III. FIELD EMISSION

A. Field emission of an individual TiO_2 nanowire

The method for sticking individual nanowires to a tungsten tip with good electrical contact has been presented elsewhere.[12] These tips can be inserted in a home-made sample holder conceived for a Topcon EM002B. Figure 3(a) illustrates the nanowire environment for *in situ* measurements: a grounded spherical electrode can be brought close to the sample using an external micrometer. Typical distances used in FE measurements are about 10 μm. Negative high voltages reaching −2 kV can be applied to the tungsten tip to extract the electrons (the voltage was limited here to −500 V). The pressure inside the TEM was 5×10^{-7} Torr which limited the FE stability due to contamination.

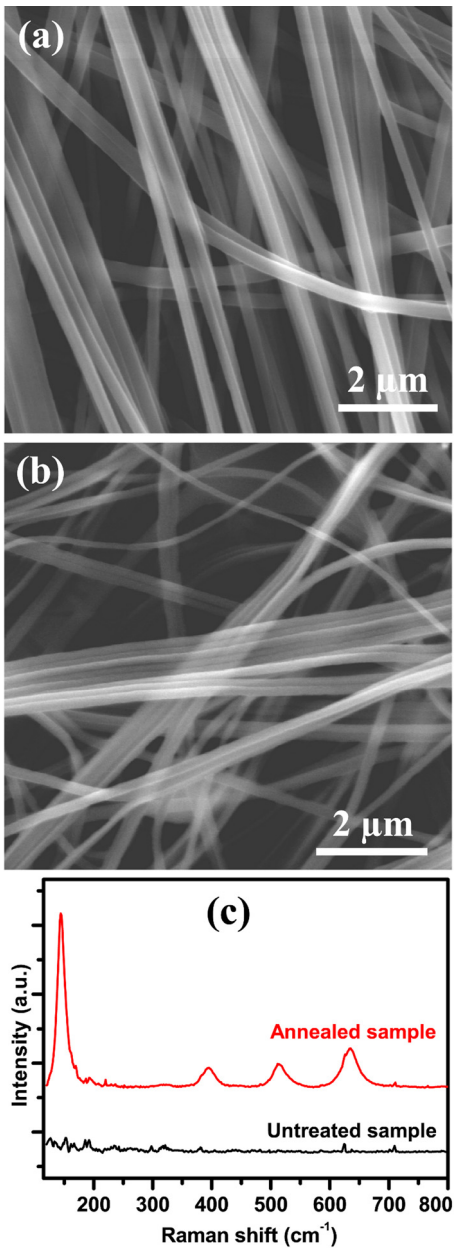

FIG. 1. (Color online) (a) SEM image of $Ti(OiPr)_4$/PVP nanowires electrospun from a solution containing 0.03 g/mL and 0.11 g/mL of PVP and $Ti(OiPr)_4$, respectively. The electric field strength was 1 kV/cm and the average diameter of these nanofibers is about 200–300 nm. (b) SEM image of the same sample after it had been calcinated in air at 500 °C for 4 h which reduced the diameters to 150 – 200 nm. (c) Raman spectra of the untreated (lower curve) and annealed (upper curve) bulk nanowire samples showing the transformation of the amorphous phase into the anatase phase (see text and Fig. 2).

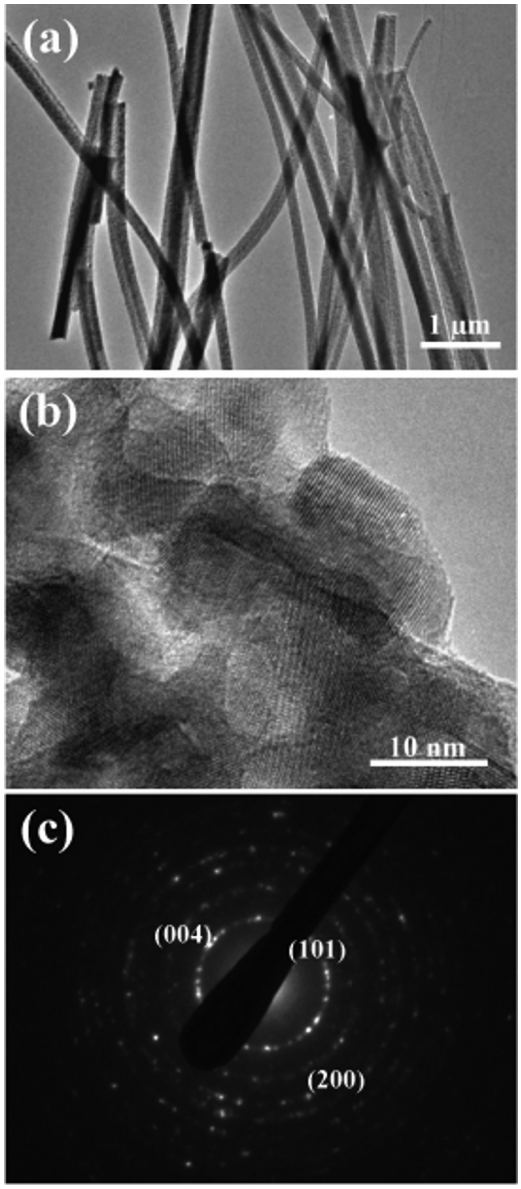

FIG. 2. (a) TEM image of the nanowires after calcination in air at 500 °C for 4 h. (b) HRTEM image of a TiO_2 nanowire showing the distinct polycrystalline structure. (c) Selected area diffraction pattern (SAED) of the nanowire with indicated (101), (004) and (200) rings representative of the Anatase structure.

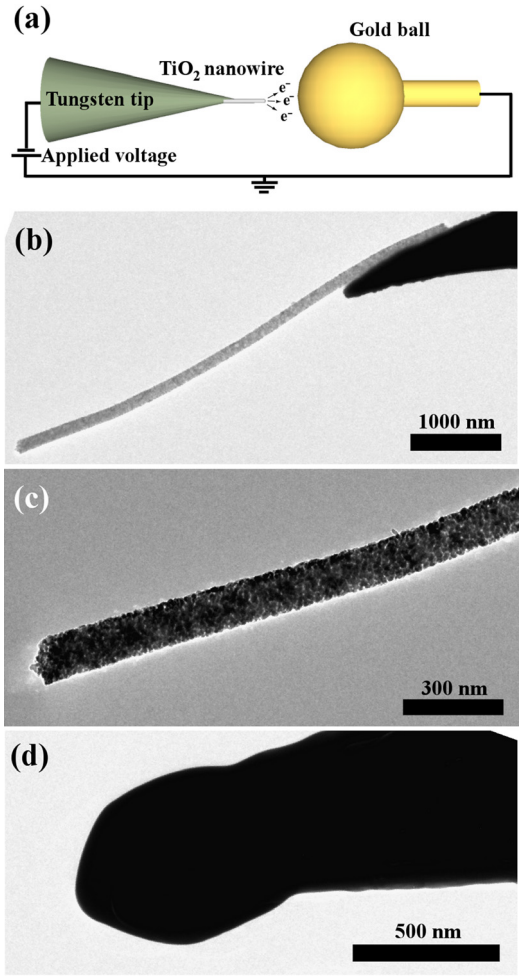

FIG. 3. (Color online) (a) Schematic of *in situ* FE measurement of an individual TiO_2 NW. The NWs are mounted on tungsten tips and placed on a micromanipulator in front of a metallic ball polarized at a positive voltage. (b) TEM image of the second sample (diameter $\phi = 150$ nm and length $L = 4\ \mu$m) for FE study. (c) TEM image of the extremity of the wire after several I-V measurements. No modification of the apex has been observed. (d) Picture of the melted tungsten tip after the rapid current runaway. The rounded shape at the extremity is due to the tungsten melting during the runaway.

As previously stated, the aim of these FE studies on individual TiO_2 nanowires was to focus on several questions concerning the general performance of such structures for FE, particularly the following points:

(1) *Mechanical resistance*. The strong electric field necessary for FE also induces a strong electrostatic longitudinal mechanical force that scales as the square of the electric field. The axial electrostatic stress can be estimated to be $1/2\ \varepsilon_0\ E^2$ which, for an electric field of 3 V/nm (typical for FE) gives a stress of 4×10^7 Pa. For our TiO_2 nanowires composed of interconnected nanocrystals, this can lead to the tearing off of nanocrystals at the nanowire end or to its rupture.

(2) *Emission mechanism*. Field emission from metallic surfaces is simple, well understood and described by the well-known Fowler-Nordheim equation,[13] but emission from semiconductors is much more complex. The work function and the field amplification factor, β, that characterizes the emitter geometry are still important parameters, but large field penetration controlled by the doping can occur in well-prepared highly crystalline emitters due to insufficient carrier concentrations and this can create large voltage drops, ΔV, and strong current saturation effects similar to reverse biased diodes. In addition, the presence of surface overlayers and contamination or surface states provide paths for leakage currents that can dominate the transport, leading generally to quasi-metallic behavior with more or less linear FN plots and a moderate voltage drop along the nanowire. Obtaining clean nanowires for FE is quite difficult and minimally requires heat treatments, good UHV conditions and ion bombardment so that, for our TiO_2 nanowires or for other nanowire FE studies, it is highly probable that the emission is controlled by the surface leakage currents.

(3) *Heating process*. Large voltage drops reaching tens to hundreds of volts can occur along semiconducting nanowires during FE which can lead to significant Joule dissipation (I ΔV) even at moderate currents and, in turn, can lead to strong temperature rises. This temperature increase depends on the geometric parameters (length and radius) and fundamental properties (thermal conductivity) of the nanowire.[14] Measurements on carbon nanotubes (CNTs) have shown heating up to 2000 K,[15,16] and that this heating phenomenon is an intrinsic limitation for the emission current.

Our approach here was to slowly increase the voltage and emission current and follow nanowire structural transformations, breakage or eventual destruction. The I-V characteristics were monitored with the help of software controlled current thresholds that allow, to a certain degree, control of rapid sample transformations.

The first sample of length 4.3 μm and diameter 130 nm had $I_{FE} = 1$ nA for ~280 V. The emission was noisy, as is expected for a nonheated sample in low vacuum because mobile adsorbates vary the tunnel barrier,[17] but was quite reproducible. We did not observe mechanical breakage or the removal of nanocrystallites from the end of the NW. Measurements made with or without electron illumination at 200 kV were similar or indistinguishable for this level of current stability. Increasing the voltage and emission led rapidly to the destruction of the nanowire for emission currents above 100 nA. We observed a sudden current increase, which was too rapid for the software to decrease the applied voltage, and the sample was destroyed. The tungsten tip appeared to have melted at the extremity which is a clear signature of current and temperature runaway. In comparison, experiments where nanowires are torn off from the tungsten tip by the electrostatic forces are not accompanied by the tungsten melting.

The second tested NW of length 4 μm and radius 75 nm is presented in Fig. 3(b). The emission started around 150 V for 1 nA and the current was again unstable and fairly reproducible. Figure 3(c) shows the extremity of the NW after some FE experiments. No modifications have been observed; thus confirming the good mechanical behavior of our system. I-V measurements have been achieved [see Fig. 4(a)] at currents in the μA range and show that these nanowires can indeed sustain high current densities up to 1700 A/cm^2. However, the decrease in the slope of the FN plot at higher currents [Fig. 4(b)] is a signature of a significant voltage drop along the NW due to a large ohmic resistance along a surface layer through which leakage current dominates the transport. After several I-V cycles we observed the same behavior as for our previous NW with a significant current increase and the disappearance of the emitter and the melting of the tungsten tip [see Fig. 3(d)].

Studies on a third NW allowed for a more detailed picture of the destruction mechanism [Fig. 5, $\phi = 90$ nm, L = 3.8 μm]. The beginning of emission was identical to the previous ones with a starting voltage of 160 V for 1 nA and a noisy current. Upon increasing the current we observed a

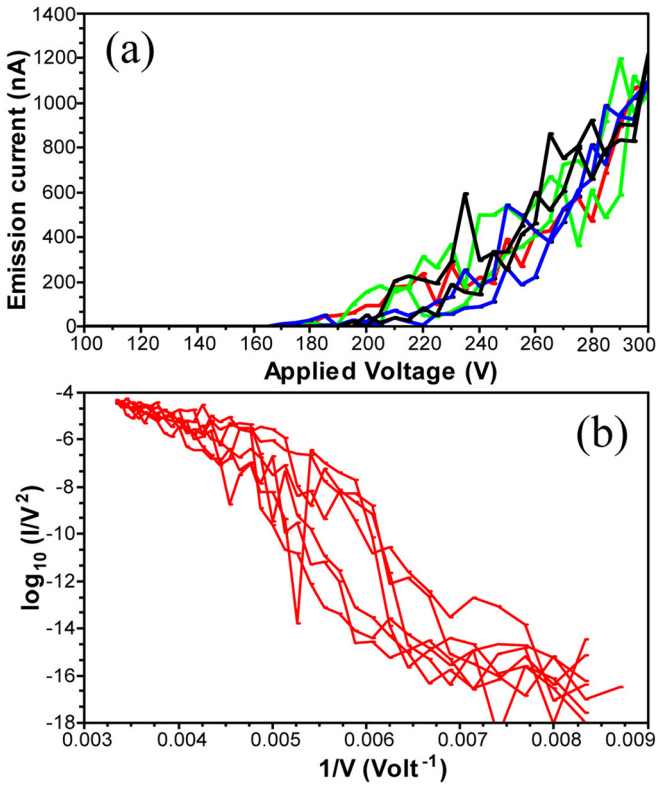

FIG. 4. (Color online) (a) TiO_2 nanowire FE characteristics. Several runs are superposed for comparison. The emission is unstable but reproducible and currents up to 1 μA can be achieved. (b) FN plot showing a characteristic slope decrease due to a voltage drop along the NW.

small change in structure at around 250 V and 800 nA [black curve in Fig. 6]. The following measurement showed nearly the same behavior at low voltage but the current increased more rapidly with voltage [see red curve in Fig. 6]. At the end of this measurement we observed a rapid modification of the nanowire extremity, accompanied simultaneously by a significant FE current increase. Images of the extremity before and after this modification are presented in Fig. 7 where we see clearly the disappearance of the nanocrystals while the overall shape remains unmodified. Observations along the length show that these modifications occurred in the last 20% of the NW length with the nanocrystalline structure being conserved for the rest of the length as can be seen in Fig. 7(c) where the region near the contact with the

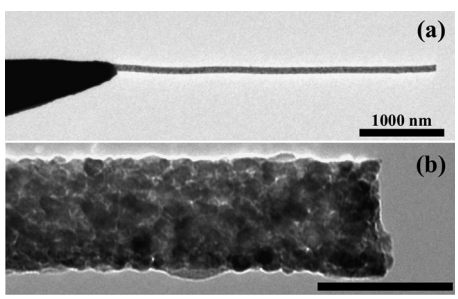

FIG. 5. (a) TEM image of as-prepared sample 3 before FE. (b) TEM image of the apex of the wire before modification (scale bar corresponds to 100 nm).

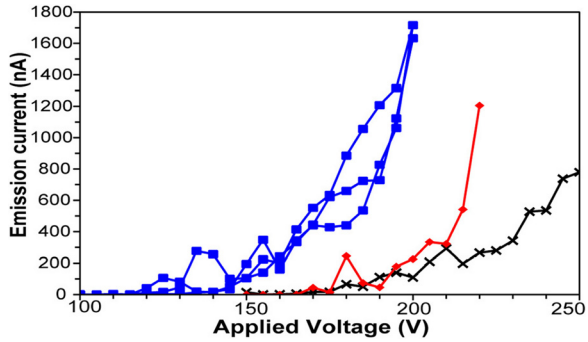

FIG. 6. (Color online) I-V curves obtained on sample presented in Fig. 5 before modification [cross marker (×)], after small change [diamond marker (◆)] and after the large modification [square marker (□)] shown in Fig. 7

tungsten tip is shown. The FE after this transition showed lower FE voltages and higher current up to 1.8 μA as seen in Fig. 6 (square marker). At this point the FE experiments were stopped in order to analyze the modification of the wire and to characterize the nature of the modification.

Structural analysis of the extremity of the wire after transformation is presented in Fig. 8. The uniform contrast at the apex of the tip following FE indicates that the TiO_2 nanocrystals have coalesced to form a few large grains near the NW apex. This was confirmed by SAED where the ring pattern obtained prior to FE had been transformed to a spot pattern characteristic of a single crystal. To try to characterize the crystallographic orientation of the large grains the sample was transferred to a double tilt sample holder but due to the limited tilt of the Topcon EM002B ultra high-resolution pole pieces ($\pm 10^\circ$ in the two axes) it was not possible to tilt the crystal into a distinctive zone axis. To further demonstrate the structural transformation at the apex of the nanowire, Fig. 8(b) shows a bright field (BF) image and its complementary tilted-beam dark field (DF) image. The DF image shows only the apex grain because the adjacent grain along the nanowire is invisible at this tilt.

Two main mechanisms can be proposed for this transition, both being thermally activated and depending on the

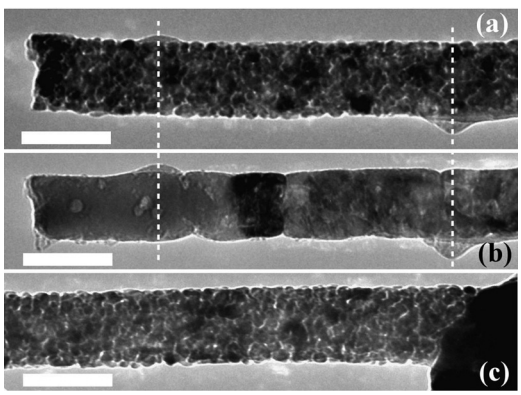

FIG. 7. (a) and (b) Comparison of the apex of the nanowire before and after the strong FE-induced modification. We see the disappearance of the small nanocrystals. This modification occurred in the last 20% of the length of the wire. (c) Image of the nanowire near the tungsten tip after modification. The structure has not been altered here. The white scale bar corresponds to 100 nm.

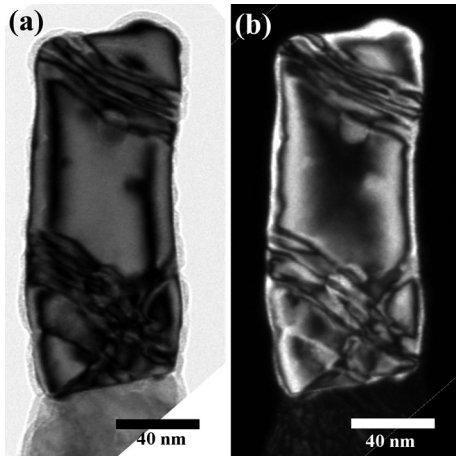

FIG. 8. (a) Bright field TEM image of the tip of a single TiO_2 nanowire after the FE annealing effect; (b) Dark field image obtained using the +**g** spot in the SAED pattern. The second grain at the bottom of the image is invisible in this DF image.

nature of the final crystals. The first could be that a phase transition occurs where anatase is converted into rutile. This phase transition and coalescence of rutile would lead to large rutile grains. The second possible mechanism is grain growth, or sintering, of anatase leading to larger anatase grains.

TEM observations did not allow us to distinguish the rutile or anatase structure of the final grains and the sample has been unfortunately destroyed during manipulation before microRaman experiments. Studies in the literature show that a phase transformation from the anatase to the rutile is likely once the nanocrystallites begin to increase in size,[18] as visible from the annealing effect seen in the TEM image in Fig. 7(b). The anatase phase has a lower surface energy than the rutile phase, which explains why the anatase is predominant for small crystallites ($<\sim$14 nm) even though the rutile phase is more stable.[19] However, once the crystallites increase in size due to the FE current annealing effect, the rutile phase may become more favorable.

B. Discussion

This transition and the associated evolution of the FE characteristics have allowed us to describe the destruction process of our nanowires. Pristine nanowires are characterized by rather significant voltage drops due to larger electrical resistances and, due to the heat generation, the temperature increases in the nanowire. Previous analysis of heating in CNTs during FE shows a nearly parabolic temperature increase along the nanowire with the highest temperature at the apex.[14] For our nanocrystalline nanowires this temperature increase leads to partial recrystallization of the wire. Considered in another way, the profile of the recrystallization can be seen as a thermometer indicating the temperature profile along the nanowire. Depending on the mechanism, temperatures between 600 and 1000 °C at the apex and in the last 20% of the NW length have been attained, with the temperature being lower for the rest of the nanowire.

This recrystallization leads to a lower voltage drop and a current increase that can be extremely rapid. As an example, we can extend the blue curve of Fig. 6 to estimate the current we would obtain for 250 V (the last point of the black curve). This current increase leads to a further temperature increase, which then starts a thermal and current runaway that explains the final destruction of the emitter and the melting of the tungsten tip. In the case of our last sample, it is possible that the current protection of our system was rapid enough to decrease the voltage and to stop the thermal runaway before sample destruction.

To confirm and characterize this thermally-activated destruction, more in-depth FE characterization is needed. Particularly, electron energy distribution (EED) measurements as a function of emission current would give the voltage drop along the nanowire and the apex temperature and; hence, corroborate the temperature increase.

An interesting prospect is the comparison between our nanowires and monocrystalline rutile nanowires.[6] The monocrystalline structure could prevent thermal and current runaway, allowing higher FE current before destruction.

IV. SUMMARY AND CONCLUSIONS

In this article, we presented the realization of individual anatase TiO_2 nanowires on W tips for FE studies. The NWs showed noisy but quite reproducible quasi-metallic emission governed by surface leakage. Currents higher than 1 μA can be obtained for individual nanowires although rapid destruction may take place. Observations indicate that this destruction is related to a thermally-activated transition that leads to rapid re-crystallization and current runaway.

ACKNOWLEDGMENTS

This work was supported by French National Research Agency (ANR) through its Nanoscience and Nanotechnology Program (Mikado, Grant No. ANR-09-NANO-018) and the 'Plateforme Nanofils et Nanotubes Lyonnaise' of the University Claude Bernard Lyon1.

[1]S. Yin, S. Uchida, Y. Fujishiro, M. Aki, and T. Sato, J. Mater. Chem. **9**, 1191 (1999).
[2]D. P. Macwan, P. N. Dave, and S. Chaturvedi, J. Mater. Sci. **46**, 3669 (2011).
[3]D. Li and Y. Xia, Nano Lett. **3**, 555 (2003).
[4]M. Miyauchi, H. Tokudome, Y. Toda, T. Kamiya, and H. Hosono, Appl. Phys. Lett. **89**, 043114 (2006).
[5]J. M. Wu, H. C. Shih, and W. T. Wu, Chem. Phys. Lett. **413**, 490 (2005).
[6]K. Huo, X. Zhang, J. Fu, G. Qian, Y. Xin, B. Zhu, H. Ni, and P. K. Chu, J. Nanosci. Nanotechnol. **9**, 3341 (2009).
[7]M. Choueib, A. Ayari, P. Vincent, S. Perisanu, and S. T. Purcell, J. Appl. Phys. **109**, 073709 (2011).
[8]M. Choueib, A. Ayari, P. Vincent, M. Bechelany, D. Cornu, and S. T. Purcell, Phys. Rev. B **79**, 075421 (2009).
[9]Z. Miao, D. Xu, J. Ouyang, X. Zhao, and Y. Tang, Nano Lett. **2**, 717 (2002).
[10]J. C. Plenet, A. Brioude, E. Bernstein, F. Lequevre, J. Dumas, and J. Mugnier, Opt. Mater. **13**, 411 (2000).
[11]A. Brioude, F. Lequevre, J. Mugnier, J. Dumas, G. Guiraud, and J. C. Plenet, J. Appl. Phys. **88**, 6187 (2000).
[12]S. Perisanu, P. Vincent, A. Ayari, M. Choueib, M. Bechelany, D. Cornu, and S. T. Purcell, Appl. Phys. Lett. **90**, 043113 (2007).
[13]R. H. Fowler and L. W. Nordheim, Proc. Soc. London, Ser. A **119**, 173 (1928).
[14]P. Vincent, S. T. Purcell, C. Journet, and V. T. Binh, Phys. Rev. B **66**, 075406 (2002).
[15]S. T. Purcell, P. Vincent, C. Journet, and V. T. Binh, Phys. Rev. Lett. **88**, 105502 (2002).
[16]S. T. Purcell, P. Vincent, M. Rodriguez, C. Journet, S. Vignoli, D. Guillot, and A. Ayari, Chem. Vap. Deposition **12**, 331 (2006).
[17]R. Gomer, *Field Emission and Field Ionization* (AIP, New York, 1993).
[18]X. Z. Ding and X. H. Liu, J. Mater. Res. **13**, 2556 (1998).
[19]H. Zhang, and J. F. Banfield, J. Mater. Chem. **8**, 2073 (1998).